Safety and Homing of Human Dental Pulp Stromal Cells in Head and Neck Cancer

Greet Merckx
Universiteit Hasselt Faculteit Geneeskunde en Levenswetenschappen https://orcid.org/0000-0003-4052-3773

Melissa Lo Monaco
Universiteit Hasselt Faculteit Geneeskunde en Levenswetenschappen

Ivo Lambrichts
Universiteit Hasselt Faculteit Geneeskunde en Levenswetenschappen

Uwe Himmelreich
KU Leuven Faculty of Medicine: Katholieke Universiteit Leuven Faculteit Geneeskunde

Annelies Bronckaers (annelies.bronckaers@uhasselt.be)
UHasselt – Hasselt University, Faculty of Medicine and Life Sciences, Biomedical Research Institute (BIOMED), Group of Cardio & Organ Systems (COS), Agoralaan, 3590 Diepenbeek, Belgium.
https://orcid.org/0000-0001-8969-873X

Esther Wolfs
Universiteit Hasselt Faculteit Geneeskunde en Levenswetenschappen

---

Research

Keywords: human dental pulp stromal cells, head and neck cancer, tumour homing, angiogenesis, epithelial-to-mesenchymal transition, cell survival, xenograft mouse model

Posted Date: September 18th, 2020

DOI: https://doi.org/10.21203/rs.3.rs-76749/v1

Version of Record: A version of this preprint was published at Stem Cell Reviews and Reports on April 6th, 2021. See the published version at https://doi.org/10.1007/s12015-021-10159-1.

Abstract

Background: Head and neck cancer (HNC) is one of the most common cancers, associated with a huge mortality and morbidity. In order to improve patient outcomes, more efficient and targeted therapies are essential. Bone marrow-derived mesenchymal stromal cells (BM-MSCs) express tumour homing capacity, which could be exploited to target anti-cancer drug delivery to the tumour region and reduce adverse side-effects. Nevertheless, dental pulp stromal cells (DPSCs), an MSC-like population present in teeth, could offer important clinical benefits because of their easy isolation and superior proliferation compared to BM-MSCs. Therefore, we aimed to elucidate the tumour homing and safe usage of DPSCs to treat HNC.

Methods: The *in vivo* survival as well as the effect of intratumourally administered DPSCs on tumour aggressiveness was tested in a HNC xenograft mouse model by using bioluminescence imaging (BLI), (immuno)histology and qRT-PCR. Furthermore, the *in vitro* and *in vivo* tumour homing capacity of DPSCs towards a HNC cell line were evaluated by a transwell migration assay and BLI, respectively.

Results: Intratumourally injected DPSCs survived for at least two weeks in the tumour micro-environment and had no significant influence on tumour morphology, growth, angiogenesis and epithelial-to-mesenchymal transition. In addition, DPSCs migrated towards tumour cells *in vitro*, which could not be confirmed after their *in vivo* intravenous, intraperitoneal or peritumoural injection under the tested experimental conditions.

Conclusions: Our research suggests that intratumourally delivered DPSCs might be used as safe factories for the continuous delivery of anti-cancer drugs in HNC. Nevertheless, further optimization as well as efficacy studies are necessary to understand and improve *in vivo* tumour homing and determine the optimal experimental set-up of stem cell-based cancer therapies, including dosing and timing.

1. Background

Head and neck cancer (HNC) is the eighth most common cancer type worldwide with a yearly incidence rate of 835,000 cases (1). HNC is a generic term for all cancers originating from the upper aerodigestive tract, including the nasal and oral cavity, pharynx and larynx (2). The most prominent histological subtype (> 90% of all HNC types) is head and neck squamous cell carcinoma (HNSCC), derived from the squamous mucosa cells in the upper aerodigestive tract (3). Incidence of HNC strongly depends on country, age, gender and cancer subtype (4), which is related to different exposure to associated risk factors, including smoking (5), alcohol (6) and Human Papilloma Virus infections (7). The classical therapeutic strategies of surgery, chemotherapy, radiotherapy or a combination are associated with a low survival rate of only 33 – 63% after five years, depending on the tumour site (8). In addition, high morbidity is induced by complications of these therapies, such as disturbed aesthetics, sensory deficits and functional problems with eating and speech, since tumours are located on difficult attainable and important organs (9).

Therefore, alternative targeted therapies with less adverse side-effects and better functional outcomes are essential to treat HNC. A promising strategy is the use of mesenchymal stromal cells (MSCs) as therapeutic vehicles for the delivery of anti-tumour drugs or therapeutic genes. These stem cells express a specific *in vitro* and *in vivo* tropism towards injury and tumour sites under the influence of secreted chemotactic mediators, including stromal cell-derived factor-1 (SDF-1) (10–17). Reciprocal communication between tumour cells and MSCs is mediated by paracrine extracellular vesicles (EVs), growth factors, cytokines and chemokines, and direct cell-cell contact (18). The resulting effect of this bidirectional interaction on tumour growth and aggressiveness is controversial (19, 20). Some studies indicate that MSCs promote tumour progression by immunosuppression and stimulation of cell survival, proliferation, angiogenesis, epithelial-to-mesenchymal transition (EMT), invasion and metastasis (21–26). In contrast, a tumour-suppressing capacity has been ascribed to MSCs via the inhibition of angiogenesis, tumour growth, invasion and metastasis, and via exerting pro-inflammatory effects (27–32).

While these *in vitro* and *in vivo* migration and safety data were mainly obtained on bone marrow-derived MSCs (BM-MSCs), these multipotent stem cells can be isolated from various other tissue sources, including adipose tissue (33, 34), umbilical cord (35) and dental soft tissues (36). Comparative studies showed significant differences in tumour homing capacity, depending on MSC origin, with a slower and more limited potency for BM-MSCs (37). Moreover, their invasive isolation and restricted proliferation capacity complicate their clinical use compared to other MSC types (38). Dental pulp stromal cells (DPSCs), an MSC subtype present in the tooth pulp, have been suggested as a beneficial alternative (36, 39). Nevertheless, studies on their tumour homing capacity and tumour-promoting or -suppressing effects are currently restricted.

Therefore, the aim of this study was to elucidate whether DPSCs can be used as vehicles for targeted delivery of anti-cancer therapies in a safe way to treat HNSCC. The impact of DPSCs on tumour growth, angiogenesis, EMT and stem cell survival was monitored *in vivo* over time in mice HNSCC xenografts using bioluminescence imaging (BLI), quantitative reverse transcriptase polymerase chain reaction (qRT-PCR) and (immuno)histology. Furthermore, *in vitro* tropism of DPSCs towards the HNSCC FaDu cell line was assessed in a transwell migration assay, while *in vivo* biodistribution was studied in a HNSCC mouse model by BLI. To our knowledge, this is the first study that evaluated both *in vivo* safety and homing capacity of DPSCs in HNC.

2. Methods

2.1 Cell Isolation and Culture

Human DPSCs (hDPSCs) were isolated from dental pulp tissue derived from wisdom teeth of healthy donors (n = 24, age 14 – 23, both sexes) undergoing tooth extraction for orthodontic or therapeutic reasons in Ziekenhuis Oost-Limburg (ZOL, Genk, Belgium). The explant outgrowth isolation method was applied as previously described (40). Stem cells were cultured in alpha modified Minimum Essential

Medium (α-MEM, Sigma-Aldrich, St-Louis, MO, USA), enriched with 10% heat-inactivated foetal bovine serum (FBS, Biowest, Nuaillé, France), 2 mM l-glutamine, 100 U/mL penicillin and 100 µg/mL streptomycin (Sigma-Aldrich). Pooled DPSCs of three donors were transduced with a lentiviral vector encoding Firefly luciferase (Fluc), enhanced green fluorescent protein (eGFP) and a blasticidin resistance cassette. After transduction, stably expressing cells were selected with blasticidin (10 µg/mL, InvivoGen, Toulouse, France). Stem cells were used until passage 15.

The FaDu tumour cell line, a human HNSCC cell line of the hypopharynx, was purchased from the American Type Culture Collection (ATCC, HTB-43, Wesel, Germany) and cultured in Dulbecco's Modified Eagle Medium, high-glucose (DMEM, Sigma-Aldrich), supplemented with 10% heat-inactivated FBS, 100 U/mL penicillin and 100 µg/mL streptomycin.

All cells were monthly screened for mycoplasma infections with the PlasmoTest™ kit (InvivoGen).

2.2 Flow Cytometry

The percentage of eGFP-positive DPSCs was first quantified by flow cytometric analysis. Hence, naïve and transduced DPSCs were rinsed twice in FACS buffer (2% FBS in phosphate buffered saline (PBS, Lonza, Walkersville, MD, USA)) and analysed by the FACSCalibur equipped with CellQuest Pro Software (BD, Erembodegem, Belgium) for 5,000 or 10,000 events.

2.3 Immunofluorescence

Protein expression of eGFP by transduced DPSCs was further analysed by immunofluorescent stainings. Cells were seeded on coverslips and fixed with 4% paraformaldehyde (PFA). Unspecific binding sites were blocked in serum-free Blocking Buffer (Dako, Heverlee, Belgium) for 20 min at room temperature, after permeabilization in 0.05% Triton (Sigma-Aldrich) in PBS during 30 min at 4 °C. Primary polyclonal rabbit anti-GFP antibody (0.5 µg/mL, #ab6556, Abcam, Cambridge, UK) was incubated overnight at 4 °C. Alexa Fluor 555-labelled secondary antibody goat anti-rabbit (4 µg/mL, #A21430, Thermo Fisher Scientific, Erembodegem, Belgium) was incubated for 30 min and nuclei were stained with 4',6-diamidino-2-phenylindole (DAPI, 0.1 µg/mL, Thermo Fisher Scientific) during 10 min at room temperature in the dark. Negative control samples, omitted of primary antibody, were included. Coverslips were mounted by Fluoromount-G™ (Thermo Fisher Scientific) and pictures were taken by the Leica DM4000 B Microscope (Leica Microsystems, Wetzlar, Germany) at a final magnification of 200 × and 400×.

2.4 *In Vivo* HNSCC Mouse Model

Eight-week-old female Hsd:Athymic Nude-Foxn1^{nu} mice (Harlan Laboratories, Indianapolis, IN, USA) were subcutaneously inoculated with 1×10^6 FaDu cells in both flanks at the level of the shoulder. Tumour cells were resuspended in 50 µL serum-free DMEM medium and 50 µL growth factor-reduced Matrigel (Corning, Lasne, Belgium). After 10 days, 1×10^6 DPSCs in 50 µL serum-free α-MEM medium were directly injected into one tumour per mice, while 50 µL serum-free medium was added to the contralateral control tumour. In a second study, animals received a single injection of 1×10^6 FaDu cells in the right flank and

were inoculated with 1×10^6 DPSCs by an intravenous, intraperitoneal, peritumoural or intratumoural injection after 10 days. Tumour growth, stem cell survival and biodistribution were monitored for 2 – 4 weeks until humane endpoints were reached. Mice were euthanized by cervical dislocation and tumours were dissected for qRT-PCR and (immuno)histology.

2.4.1 Tumour Growth Measurements

The effect of DPSCs on HNSCC growth was studied by monitoring the tumour size after intratumoural stem cell injection. The tumour size was measured blindly twice a week by a calliper. Tumour volume (mm^3) was calculated by the formula $0.5 \times a^2 \times b$, with a and b representing the width and length of the tumour in mm, respectively (41).

2.4.2 Bioluminescence Imaging (BLI)

The survival and biodistribution of Fluc-expressing DPSCs were monitored noninvasively 24 h, 7 days and 14 days after their injection by BLI. Mice were anesthetized with isoflurane (2% in 100% oxygen) at a flow rate of 2 L/min. D-luciferin (15 mg/mL in PBS, Promega, Leiden, The Netherlands) was intravenously injected at a dose of 126 mg/kg body weight. Consecutive frames were acquired using an IVIS Spectrum (PerkinElmer, Waltham, MA, USA) until the maximum signal intensity was achieved. Images were processed using the Living Image Software (PerkinElmer). Regions of interest (ROIs) were marked around the BLI signal and the total photon flux (p/s) within this area was quantified by Aura Imaging Software (Spectral Instruments Imaging, Tucson, AZ, USA).

2.4.3 Quantitative reverse transcriptase polymerase chain reaction (qRT-PCR)

Tumour expression of angiogenic- and EMT-related genes was analysed in mice bearing two contralateral tumours by the StepOne Plus PCR system (Applied Biosystems, Carlsbad, CA, USA). Tumours were snap frozen and stored at − 80 °C until further processing. After shredding of the tissues, total RNA was extracted by the RNeasy Plus Mini Kit (Qiagen, Venlo, The Netherlands), following the manufacturer's instructions. The concentration and purity of the isolated RNA were measured by Nanodrop spectrophotometry (NanoDrop 2000, Thermo Fisher Scientific) at 260 nm, 260/230 nm and 260/280 nm ratio, respectively. cDNA was generated from 500 ng RNA template with the qScript cDNA SuperMix (Quanta Biosciences, Gaithersburg, MD, USA), according to the manufacturer's protocol. qPCR mixes contained 0.3 µL forward and reverse primers (10 µM, Eurogentec, Seraing, Belgium) (Table 1), 5 µL FAST Sybr Green Master Mix (Applied Biosystems) and 2 µL cDNA (1/10 diluted in RNase-free water) in a final reaction volume of 10 µL. The amplification protocol consisted of an initial denaturation step at 95 °C during 20 s, 40 cycli at 95 °C for 3 s and 60 °C during 30 s, followed by one cycle at 95 °C during 15 s and a final elongation step of 60 s at 60 °C. The melting curve was analysed by a gradual increase in temperature to 95 °C (+ 0.3 °C/15 s). Data were normalized to the endogenous expression of housekeeping genes human ribosomal protein L13a (RPL13a) and cyclophilin A (cyc A) and mouse yrosine 3-monooxygenase/tryptophan 5-monooxygenase activation protein zeta (Ywhaz) and

hypoxanthine phosphoribosyltransferase 1 (HPRT1). A non-template control was included for every gene. Data were analysed with the StepOne Software 2.3 (Applied Biosystems).

Table 1
Overview of primers used for qRT-PCR.

Gene		Primer sequence 5'-3'
Mouse CD31	Forward	GAC-TCA-CGC-TGG-TGC-TCT-ATG-C
	Reverse	TCA-GTT-GCT-GCC-CAT-TCA-TCA
Mouse VEGF	Forward	CTC-CAG-GGC-TTC-ATC-GTT-A
	Reverse	CAG-AAG-GAG-AGC-AGA-AGT-CC
Human TWIST	Forward	CAT-CCT-CAC-ACC-TCT-GCA-TTC-T
	Reverse	ACT-ATG-GTT-TTG-CAG-GCC-AGT-T
Human SNAIL2	Forward	CTT-TTT-CTT-GCC-CTC-ACT-GC
	Reverse	GCT-TCG-GAG-TGA-AGA-AAT-GC
Human α-SMA	Forward	GCA-CCC-CTG-AAC-CCC-AAG-GC
	Reverse	GCA-CGA-TGC-CAG-TTG-TGC-GT
Human RPL13a	Forward	AAG-TTG-AAG-TAC-CTG-GCT-TTC
	Reverse	GCC-GTC-AAA-CAC-CTT-GAG-AC
Human Cyc A	Forward	AGA-CTG-AGT-GGT-TGG-ATG-GC
	Reverse	TCG-AGT-TGT-CCA-CAG-TCA-GC
Mouse HPRT1	Forward	CTC-ATG-GAC-TGA-TTA-TGG-ACA-GGA-C
	Reverse	GCA-GGT-CAG-CAA-AGA-ACT-TA-TAG-CC
Mouse Ywhaz	Forward	GCA-ACG-ATG-TAC-TGT-CTC-TTT-TGG
	Reverse	GTC-CAC-AAT-TCC-TTT-CTT-GTC-ATC

α-SMA: *alpha-smooth muscle actin;* Cyc A: *cyclophilin A;* HPRT1: *hypoxanthine phosphoribosyltransferase 1;* RPL13a: *ribosomal protein L13a;* VEGF: *vascular endothelial growth factor;* Ywhaz: *yrosine 3-monooxygenase/tryptophan 5-monooxygenase activation protein zeta*

2.4.4 Histology and Immunohistochemistry

Tumours were fixed in 4% PFA for 48 h at 4 °C and the presence of blood vessels and EMT was evaluated. Following antigen retrieval in 10% citrate buffer (Dako), endogenous peroxidase activity was inhibited. In addition, aspecific binding sites were blocked in serum-free Blocking Buffer for 20 min at room temperature. Tissues were incubated with primary monoclonal antibodies rabbit anti-mouse/human CD146 (2.5 µg/mL, EPR3208, #ab75769, Abcam), mouse anti-human alpha-smooth

muscle actin (α-SMA, ready-to-use, ASM-1, #PA0943, Leica Biosystems, Diegem, Belgium) or mouse anti-human Snail-2 (2 µg/mL, A-7, #sc-166476, Santa Cruz, Heidelberg, Germany) for 1 h, followed by secondary antibody horseradish peroxidase (HRP) labelled goat anti-rabbit (ready-to-use, #K4002, Dako) or anti-mouse (0.5 mM, #P0447, Dako) during 30 min at room temperature. Protein expression was visualized by 3,3'-Diaminobenzidine (DAB, Dako), according to the manufacturer's instructions. Nuclei were counterstained with Mayer's haematoxylin for 8 min at room temperature. Negative controls in which primary antibodies were omitted were included. Tumour morphology was evaluated by haematoxylin-eosin (H&E) and Masson's trichrome stainings. The H&E staining was performed by incubation of tumour sections with haematoxylin for 8 min and eosin during 3 min at room temperature. For the Masson's trichrome staining, tissues were stained with haematoxylin and Ponceau/Fuchsine for 10 min and 5 min, respectively. This was followed by incubation with 1% phosphomolybdic acid, aniline blue and again 1% phosphomolybdic acid during 5 min and finally 1% acetic acid for 2 min. Tissue sections were rehydrated, enclosed with DPX mounting medium (Merck, Darmstadt, Germany) and scanned by the Mirax digital slide scanner or Axio Scan.Z1 (Carl Zeiss, Jena, Germany). The percentage of positive cells was quantified by Axiovision 4.6 Software (Carl Zeiss) or ImageJ Software (National Institutes of Health (NIH), Bethesda, MD, USA), respectively.

2.5 Transwell Migration Assay

The *in vitro* tumour homing capacity of DPSCs was studied by a Boyden chamber migration assay. FaDu cells were seeded at a density of 25,000 cells/cm² in a 24-well plate in their standard culture medium. After overnight adherence, cells were rinsed in PBS and 500 µL serum-free α-MEM medium was added. 24 h later, 50,000 or 100,000 DPSCs were seeded in 24-Transwell inserts (pore size 8.0 µm, Corning) in 300 µL serum-free α-MEM medium and placed in the wells containing tumour cells. Medium with or without 10% FBS in the bottom wells was used as positive and negative control, respectively. After 24 h, DPSCs were fixed in 4% PFA and stained with 0.1% crystal violet (Sigma-Aldrich) in 70% ethanol. Non-migrated cells on the upper side of the insert were swept away by a cotton swab. Representative pictures of transmigrated DPSCs on the lower side were captured by a Nikon eclipse TS100 inverted microscope with Jenoptik ProgRes C3 camera (Jenoptik, Jena, Germany) at a final magnification of 100×. Alternatively, migrated DPSCs were dissociated and stained with 1.67 mM calcein acetoxymethyl esther (BD) in Non-Enzymatic Cell Dissociation Solution Buffer (Sigma-Aldrich). The resulting fluorescent signal was measured by a FLUOstar Omega plate reader (excitation: 485 nm, emission: 520 nm, BMG LABTECH, Ortenberg, Germany). The absolute number of transmigrated stem cells was quantified based on a standard curve.

2.6 Statistical Analysis

All quantitative data were expressed as mean ± standard error of the mean (S.E.M.). Statistical analysis was performed with GraphPad Prism 8 software (Graphpad Software, La Jolla, CA, USA). After testing data normality by the D'Agostino and Pearson omnibus normality test, the Mann-Whitney U test was performed to compare two groups. Tumour growth over time was statistically analysed using the two-way ANOVA and Sidak's multiple comparisons test. For the comparison of multiple groups, the one-way

ANOVA test combined with the Dunnett's multiple comparisons test was used. P values below 0.05 were considered statistically significant.

3. Results

3.1 *In Vivo* Survival of DPSCs in the Tumour Microenvironment

In order to evaluate the therapeutic potential of DPSCs as carriers to specifically deliver anti-cancer treatment in the tumour region, we investigated stem cell survival and biodistribution over time using BLI after intratumoural stem cell injection (Fig. 1). Therefore, immune-deficient mice bearing two HNSCC xenografts were injected with control medium or Fluc- and eGFP-expressing DPSCs. Successful lentiviral transduction of DPSCs was confirmed by immunofluorescence and flow cytometry, in which 97.91 ± 0.16% of the transduced DPSC population was eGFP positive (see **Additional file 1**). Following intratumoural injection in the mouse xenograft model, DPSCs were detectable in the tumours for two weeks, while no BLI signal could be measured in the control tumours on the contralateral side (Fig. 1A). Quantification of the total photon flux showed a decrease in stem cell survival after 14 days to about 25%, ranging from $4.2 \times 10^6 \pm 1.8 \times 10^6$ p/s after 24 h, to $4.6 \times 10^6 \pm 2.8 \times 10^6$ p/s and $1.2 \times 10^6 \pm 3.8 \times 10^5$ p/s after 7 and 14 days, respectively (Fig. 1B). These data suggest the survival and *in situ* persistence of intratumourally injected DPSCs in the applied HNC mouse model. In addition, no detectable BLI signal was noticed outside the original engraftment zone, indicating that stem cells have not migrated towards other tissues and organs.

3.2 No Significant Effect of Transplanted DPSCs on the Morphology, Growth, EMT and Vascularization of Mouse HNSCC Grafts

We evaluated whether DPSCs can be used safely as a cell-based tumour therapy. Therefore, the impact of DPSCs injected directly into the tumour on cancer aggressiveness was studied. First, tumour growth in mice bearing two contralateral tumours was followed-up over time. Although a tendency for faster growth was observed in DPSC-injected tumours, no significant difference in tumour volume could be measured during the first 14 days after stem cell transplantation (561.35 ± 98.74 mm³ (DPSCs) vs. 420.53 ± 57.35 mm³ (control) at endpoint) (Fig. 2A). To exclude potential paracrine effects of transplanted DPSCs on the opposite control tumour, the same experiment was repeated in single tumour-bearing mice. Analogous results were observed on tumour growth for the first three weeks, with no significant effect of DPSC injection (1108.42 ± 164.61 mm³ (DPSCs) vs. 872.31 ± 82.94 mm³ (control) at endpoint) (Fig. 2B). H&E stainings revealed a similar morphology for both DPSC- and non-injected HNC tumours, characterized by a heterogeneous appearance with high cellular density (Fig. 2C). In addition, tumour cells were embedded in a connective tissue-rich matrix as demonstrated by a Masson's trichrome staining (Fig. 2D).

In addition, the effect of DPSCs on tumour angiogenesis and EMT was tested after 14 days by measuring the gene and protein expression levels of process-related molecules (Figs. 3 and 4). Control and DPSC-

injected tumours expressed similar levels of the vascular-related genes CD31 and vascular endothelial growth factor (VEGF) (0.68 ± 0.28 (CD31) and 0.86 ± 0.21 (VEGF)) (Fig. 3A). Furthermore, blood vessels were microscopically visualized in histological tumour sections by immunohistochemical staining for the endothelial marker CD146. Quantification of the percentage CD146-positive cells in the examined tissue area could not show a difference between both conditions (2.20 ± 0.32% (DPSCs) vs. 2.21 ± 0.69% (control)) (Fig. 3B).

Similar results were observed for the expression of EMT-supporting factors in HNSCC xenografts. Gene expression of TWIST, SNAIL2 and α-SMA remained unchanged following the injection of DPSCs (0.81 ± 0.33 (TWIST), 0.95 ± 0.40 (SNAIL2), 0.66 ± 0.12 (α-SMA)) (Fig. 4A). These findings were confirmed on the protein level for α-SMA (Fig. 4B) and Snail-2 (Fig. 4C) by immunohistological stainings. Hence, no significant differences between control and DPSC-injected tumours could be observed (α-SMA: 0.18 ± 0.06% (DPSCs) vs. 0.17 ± 0.06% (control), Snail-2: 21.71 ± 11.41% (DPSCs) vs. 25.53 ± 11.87% (control)). While the Snail-2 protein was distributed throughout the tumour, α-SMA expression was very limited and particularly concentrated in the smooth muscle cells around the blood vessels.

To conclude, DPSCs did not significantly influence tumour growth, morphology, neovascularization nor EMT in a mouse HNSCC xenograft model under the given conditions.

3.3 *In vitro* and *in vivo* tumour homing capacity of DPSCs

The potential of DPSCs to specifically home towards HNSCC tumours was tested. The tumour tropism of DPSCs was first studied in an *in vitro* transwell migration assay (Fig. 5A). Significant stem cell migration towards the FaDu tumour cell line could be observed (12,616 ± 1,694 vs. 2,501 ± 661 migrated cells) (Fig. 5B). Moreover, transduction of DPSCs with the Fluc-eGFP lentiviral vector had no effect on their tumour homing potency (data not shown).

In order to study the *in vivo* tropism of DPSCs, Fluc-expressing stem cells were injected intravenously, intraperitoneally or peritumourally in a FaDu xenograft mouse model. Cell biodistribution was followed-up during two weeks by BLI. Intravenously administered DPSCs were entrapped in the lungs of all animals after 24 h, with the signal persisting for two weeks (Fig. 5C). After intraperitoneal injection, the detection of DPSCs was restricted to the abdominal cavity. In one out of three mice no BLI signal could be measured, suggesting an experimental error (Fig. 5D). Finally, peritumourally administered DPSCs persisted at the injection site mediocaudal of the tumour xenograft (Fig. 5E). In all conditions, the measured BLI signal gradually decreased over time, suggesting stem cell death. While the signal was already strongly decreased at day 7 after intravenous delivery, this decline was only observed after 14 days in the intraperitoneally and peritumourally injected mice.

To conclude, despite their *in vitro* migration potential towards a HNSCC cell line, a first pilot experiment in an immune-deficient HNSCC xenograft mouse model could not reveal *in vivo* homing of DPSCs following diverse administration routes.

4. Discussion

HNC remains one of the ten most common cancer types worldwide, associated with a high morbidity and mortality (1, 8, 9). More efficient and targeted therapies are required to reduce this disease burden. Therefore, this study aimed to elucidate the potential safe use of DPSCs as therapeutic carriers to treat HNC.

As a first objective, the biological behaviour of DPSCs directly injected in a mouse HNSCC xenograft model was evaluated. Stem cells were able to survive for at least two weeks in the tumour environment. After 14 days, their survival was decreased to about 25%. Moreover, DPSCs did not have a significant effect on tumour growth, EMT and angiogenesis. The EMT is a cellular mechanism associated with the loss of epithelial properties and the transformation towards a more migratory mesenchymal cell type by the reduction of cell-cell contacts, which enhances tumour progression, invasion and metastasis (22, 42). In addition, angiogenesis increases the oxygen and nutrient supply to stimulate tumour growth and metastasis (43, 44).

The number of previous studies on the safe use of DPSCs as HNC therapy is limited to Hanyu *et al.* Similar to our results, they did not observe significant effects of hDPSC-derived conditioned medium (CM) on *in vitro* HNSCC proliferation and therapeutic sensitivity, and *in vivo* tumour growth, despite the increase in tumour VEGF secretion (45). Conflicting results on the impact of other MSC subtypes on *in vitro* and *in vivo* HNC cell proliferation, survival, migration, invasion and therapeutic sensitivity have previously been described (46–53). These effects are mediated in a direct way via differentiation of MSCs into malignant cells (54, 55), cancer-associated fibroblasts (CAFs) (56) and vascular-related cells (57, 58), or indirectly by (paracrine) interaction with immune cells (27, 59, 60), cancer stem cells (CSCs) (61–63), endothelial cells (24, 28, 64) and tumour cells (24, 30, 31, 65). For example, *in vitro* co-culture of human palatine tonsil-derived MSCs with hypopharyngeal or laryngeal squamous carcinoma cell lines inhibited cell growth, induced cell cycle arrest in the G_0/G_1 phase and apoptosis of the tumour cells in a dose-dependent way (47). Similar results were observed for hBM-MSC-derived CM with an *in vitro* decrease in FaDu cell proliferation, survival, EMT marker expression, migration and invasion, at least partially via the paracrine effects of CD109 (48). In contrast, Scherzad *et al.* and Liu *et al.* demonstrated paracrine stimulating effects of hBM-MSCs on *in vitro* and *in vivo* proliferation, viability, EMT, migration and metastasis of different HNC cell lines by interleukin-6 (IL-6) secretion and phosphoinositide-3-kinase (PI3K)/Akt signalling (50, 51). Moreover, *in vitro* 3D co-culture spheroids of human BM-MSCs or adipose tissue-derived MSCs (AT-MSCs) and HNSCC cells stimulated tumour migration and invasion via increased matrix metalloproteinase (MMP), IL-8 and VEGF expression (52, 53). Therefore, further (long-term) *in vivo* studies are required to assess whether DPSCs also not interfere with other parameters of HNSCC aggressiveness, including metastasis, invasion and therapeutic sensitivity.

In addition, the *in vitro* and *in vivo* migration capacity of DPSCs towards the FaDu HNSCC cell line was evaluated. As previously demonstrated for BM-MSCs (49, 66–68), FaDu cells displayed a significant chemoattractant effect on DPSCs in an *in vitro* transwell migration assay. Different administration routes

have already been applied to test the *in vivo* tropism of MSCs towards cancer cells. A systematic review showed that 45% of the studies used subcutaneous, 24% intravenous, 15% intratumoural and 8% intraperitoneal MSC injection, with varying results. Alternative but less frequently used routes are intramuscular and intra-arterial injections (69). Despite our positive *in vitro* transwell data, no migration of DPSCs towards FaDu tumours was observed over two weeks in an *in vivo* mouse tumour xenograft model after their intravenous, peritumoural or intraperitoneal administration. Intravenously injected DPSCs were mainly trapped in the small lung capillaries, which is a commonly described issue (70). With a diameter of 15 – 16 µm, DPSCs are slightly smaller than other MSC subtypes (17 – 18 µm) (71, 72), but still outreach the size of the narrow lung capillary network (6 – 15 µm) (73, 74). Therefore, systemic administration of MSCs is generally not recommended in cancer and other scientific research fields, since the cell numbers reaching the desired target tissue are not sufficient to induce therapeutic effects (46, 70, 75, 76). Nevertheless, gradual migration of entrapped MSCs towards tumours has been demonstrated by other researchers and systemic administration could be useful in case of lung tumours or metastases (15, 16, 67, 77). Furthermore, it cannot be excluded that MSCs captured in the lungs might play a beneficial paracrine role on distant tumours (78). After peritoneal injection, DPSCs persisted in the abdominal cavity where they could be attached to peritoneal surfaces, such as mesentery and omentum, or accumulated in spleen and lymph nodes which has been demonstrated for BM-MSCs (79). Peritumourally administered stem cells also persisted in the injection site surrounding the tumour, with no migration being observed.

Similarly, Zurmukhtashvili *et al.* studied the tropism of 1×10^6 intravenously injected mouse BM-MSCs, three weeks after establishment of human oral squamous carcinoma (1×10^6 cells) in the buccal tissue of mice. BLI revealed concentration of the stem cells in the lungs, with no signal detected in the oral cavity (46). Although Zielske *et al.* did show specific *in vivo* tropism of intravenously injected hBM-MSCs towards head and neck UMSCC1 xenografts after 3, 8 and 14 days, the number of migrated cells was relatively low compared to HT-29 colon and MDA-MB-231 breast carcinomas. Moreover, in comparison to the other tumour cell lines, MSC migration towards the head and neck tumours could not be stimulated by irradiation. The tumour cell to MSC ratio was similar to our study, but the time point of MSC injection after tumour inoculation was not clearly mentioned (77). Furthermore, Wang *et al.* showed a specific *in vivo* migration of hBM-MSCs towards hypopharyngeal carcinoma (5×10^6 FaDu cells). The stem cells were intravenously administered after one week (100,000 cells) and captured in the lungs for the first 24 hours. During the following days, BM-MSCs gradually migrated towards the subcutaneously implanted tumour until day 7, when the BLI signal could no longer be detected in these tumour-bearing mice (67). The conflicting tumour homing capacity has also been described in other animal tumour models. For example, in the study of Bianchi *et al. in vitro* migration of hBM-MSCs towards neuroblastoma cell lines was shown. Nevertheless, these results could not be confirmed *in vivo* after intravenous injection of these stem cells in mice that were inoculated with neuroblastoma cells. A small bioluminescent signal could only be detected in the lungs 8 days after their injection, which was no longer detectable after 15 days (75). In contrast, a number of other researchers successfully observed specific migration of MSCs

towards implanted tumour xenografts via diverse administration routes after a few hours to days (10, 15–17, 80). Contradictory results have also been observed in the first clinical trials (81, 82).

These conflicting data on the safety and homing of MSCs in the cancer research field could be related to MSC origin, tumour type and other experimental parameters that interfere with the MSC-tumour cross-talk. Tumours are considered chronic wounds, resulting in a strong immune response with the release of cytokines, chemokines and growth factors (83). Therefore, tumour homing is suggested to be mediated by similar mechanisms underlying MSC tropism towards inflammatory or injury sites (84). This hypothesis is supported by the stimulating effect on MSC migration following tumour destruction by irradiation (85, 86). The secretion profile of chemoattractant molecules and the resulting MSC homing vary depending on the tumour type, size, grade and inflammatory status (46, 81). Furthermore, the expression of associated chemokine receptors on MSCs depends on their tissue origin (37). Hence, the immune status of the used experimental animal model might play an important role in the observed results on MSC homing and tumour aggressiveness. As reviewed by Oloyo *et al.*, most researchers (64%) utilize immune-competent animals. Sixty-one percent of these studies observed tumour-stimulatory effects, while this was only 48% in immune-deficient or immunocompromised animal models (69). These data suggest a significant indirect interaction of MSCs with tumour cells via the immune system and notify the impact of the animal model on the observed results. Since our study was performed in athymic mice lacking T cell-mediated immune responses, further validation of our observations in immune-competent animals is essential to obtain a more significant reflection of the clinical situation. In addition, the tissue origin of MSCs has a significant impact on the tumour growth as 80% of the studies on umbilical cord-derived MSCs (UC-MSCs) show an *in vitro* or *in vivo* anti-tumour effect, compared to 36% and 43% for BM-MSCs and AT-MSCs, respectively (69). For example, *in vitro* and *in vivo* glioma progression was stimulated by AT-MSCs, but inhibited by UC-MSCs in the study of Akimoto *et al.*, which was associated with different secretion profiles of apoptotic- and angiogenesis-related factors (87). Furthermore, BM-MSCs transformed into CAFs after exposure to breast tumours in contrast to Wharton's Jelly-derived MSCs (WJ-MSCs) (88). The percentage of publications describing tumour stimulation by MSCs fluctuates from 24% in glioma models to 84% in gastric cancers and 67% in HNSCC. In addition, the *in vivo* administration route of both MSCs and tumour cells influences their reciprocal interplay. Intravenous injection of tumour cells and intraperitoneal MSC administration cause tumour reduction in 73% and 69% of the cases, respectively, while studies using subcutaneously inoculated tumours (68%) and MSCs (76%) more often observe enhanced tumour growth. The tumour homing capacity of MSCs and their eventual direct or indirect cross-talk with tumour cells are after all also dependent on the administration route (69).

Future research should focus on optimizing the *in vivo* tumour homing capacity of DPSCs in order to enable indirect stem cell delivery modes. Potential alternative administration routes include intra-arterial injection which circumvents the lung barrier and induced superior MSC homing in a glioma model compared to intravenous application (17). Furthermore, the ratio of DPSCs to tumour cells could be reduced to increase the relative availability of tumour-secreted chemotactic factors per stem cell. Although MSC tumour homing is generally observed after a few hours to days, it cannot be excluded that

DPSC migration towards HNSCC xenografts requires several weeks. However, due to the rapid growth of FaDu xenografts, longer follow-up of the animals was ethically not possible under the tested conditions of our experiment as humane endpoints had been reached. In order to prolong *in vivo* analysis of stem cell biodistribution, lower tumour cell numbers could be inoculated to slow down tumour growth and DPSCs could be injected in an earlier stage of tumour development or co-injected with tumour cells. In that case, the possible risk would be that the tumours could not produce a sustainable amount of chemokines to attract the DPSCs. Alternative approaches to enhance tumour homing could be the overexpression of important chemokine receptors (e.g., C-X-C motif chemokine receptor 4 (CXCR4)) on DPSCs or tumour irradiation which increases the release of chemoattractant molecules by tumour-associated cells.

Although the tumour-promoting or -suppressing effects and homing potential of MSCs remain controversial, preclinical studies in other tumour models show promising results for MSCs as vehicles for the continuous delivery of anti-cancer therapeutics. This hypothesis is also supported by our preliminary data on *in vivo* DPSC survival and safe interaction with tumour cells after their direct intratumoural application. Administration of MSCs genetically overexpressing tumour necrosis factor-related, apoptosis-inducing ligand (TRAIL), cytokines, angiogenic inhibitors or suicide genes reduced tumour cell viability and growth and improved survival rates in diverse animal cancer models (10, 89–91). Data on the *in vivo* therapeutic potential of DPSCs carrying anti-tumour drugs are currently scarce and requires further intensive research. A single study by Altanerova *et al.* suggested specific homing and tumour-suppressing effects for hDPSCs, genetically transduced with suicide genes and labelled by iron oxide, in a rat glioblastoma model. Nevertheless, reduction in tumour cell growth was solely demonstrated *in vitro* and the *in vivo* tropism was only based on the detection of iron oxide in the tumour region. It was not clear whether the DPSCs were still alive at that moment or that their iron oxide was taken up by other cells such as macrophages. Experiments to adequately confirm the presence of viable transplanted DPSCs were not performed (80). Salehi *et al.* demonstrated the successful loading of hDPSCs with paclitaxel, one of the most commonly used chemotherapeutics, with a better resistance to the cytotoxic effects compared to hBM-MSCs. Their *in vitro* data showed secretion of the anti-cancer drug in a time-dependent way, resulting in apoptosis in a breast cancer cell line, which sparks hope for future *in vivo* studies (92).

5. Conclusion

To conclude, our data suggest the safe use of intratumourally applied DPSCs as therapeutic vehicles for the treatment of HNSCC. Nevertheless, further long-term *in vivo* studies evaluating both the safety and efficacy of DPSCs, engineered to express anti-cancer drugs or genes, are essential. In addition, optimization of the number and timing of DPSC injection might improve their tumour homing potential and requires further analysis. Comparative studies with other MSC subtypes should also reveal whether the strong proliferative and easily isolated DPSCs are the most efficient and safe MSCs for HNC treatment, since the bidirectional interaction between MSCs and tumour cells is strongly dependent on the tissue origin of both cell types, among many other experimental conditions.

6. Abbreviations

α-MEM Minimum Essential Medium, alpha modification

α-SMA Alpha-smooth muscle actin

ATCC American Type Culture Collection

AT-MSCs Adipose tissue-derived mesenchymal stromal cells

BLI Bioluminescence imaging

BM-MSCs Bone marrow-derived mesenchymal stromal cells

CAFs Cancer-associated fibroblasts

CM Conditioned medium

CSCs Cancer stem cells

CXCR C-X-C motif chemokine receptor

Cyc A Cyclophilin A

DAB 3,3'-Diaminobenzidine

DAPI 4',6-diamidino-2-phenylindole

DMEM Dulbecco's Modified Eagle Medium

DPSCs Dental pulp stromal cells

eGFP Enhanced green fluorescent protein

EMT Epithelial-to-mesenchymal transition

EVs Extracellular vesicles

FBS Foetal bovine serum

Fluc Firefly luciferase

GFP Green fluorescent protein

H&E Haematoxylin-eosin

hBM-MSCs Human bone marrow-derived mesenchymal stromal cells

hDPSCs Human dental pulp stromal cells

HNC Head and neck cancer

HNSCC Head and neck squamous cell carcinoma

HPRT1 Hypoxanthine phosphoribosyltransferase 1

IL Interleukin

MMPs Matrix metalloproteinases

MSCs Mesenchymal stromal cells

PBS Phosphate buffered saline

PFA Paraformaldehyde

PI3K Phosphoinositide-3-kinase

(qRT-)PCR (quantitative reverse transcriptase) Polymerase chain reaction

ROIs Regions of interest

RPL13a Ribosomal protein L13a

S.E.M. Standard error of the mean

TRAIL Tumour necrosis factor-related, apoptosis-inducing ligand

UC-MSCs Umbilical cord-derived mesenchymal stromal cells

VEGF Vascular endothelial growth factor

WJ-MSCs Wharton's Jelly-derived mesenchymal stromal cells

Ywhaz Yrosine 3-monooxygenase/tryptophan 5-monooxygenase activation protein zeta

ZOL Ziekenhuis Oost-Limburg

7. Declarations

Ethics approval and consent to participate

The study protocol on DPSC isolation was approved by the medical ethical committee of Hasselt University (Hasselt, Belgium, protocol 13/0104U, date of approval 3 February 2014) and written informed

consent was obtained from the donors or guardians in case of minors. The Ethical Committee on Animal Experiments of Hasselt University (Hasselt, Belgium) and KU Leuven (Leuven, Belgium) approved the *in vivo* experimental set-up of the tumour mouse model.

Consent for publication

Not applicable.

Availability of data and materials

The datasets used and/or analysed during the current study are available from the corresponding author on reasonable request.

Competing interests

The authors declare that they have no competing interests.

Funding

G.M. was supported by 'Bijzonder Onderzoeksfonds' of Hasselt University (BOF, BOF16DOC06). M.L.M. was funded by 'Bijzonder Onderzoeksfonds' and 'Fonds Spécial de Recherche' (BOF16DOCNA02-FSR-confin UHasselt-UNamur). This research was further supported by research grants to I.L., U.H., A.B. and E.W. from the Research Foundation Flanders ('Fonds Wetenschappelijk Onderzoek Vlaanderen (FWO)', grant numbers G0C1916FWO, 1517916N and G0A7514N), BOF of Hasselt University (BOF20TT04), Limburg Cancer foundation ('Limburgs kankerfonds' LIKAF) and KU Leuven for PF 10/017 IMIR. The funding bodies played no role in study design, data collection, analysis and interpretation, or writing of the manuscript.

Author's contributions

G.M. contributed to conception, experimental design, data collection and interpretation, statistical analyses and writing of the manuscript. M.L.M., E.W. and A.B. contributed to conception, experimental design, data collection and interpretation, statistical analyses and critical revision of the manuscript. I.L. and U.H. contributed to experimental design and critical revision of the manuscript. All authors gave their approval for the final manuscript and agree to be accountable for all aspects of the work.

Acknowledgements

We would like to thank Evelyne Van Kerckhove and Jeanine Santermans for their excellent technical assistance.

8. References

1. Bray F, Ferlay J, Soerjomataram I, Siegel RL, Torre LA, Jemal A. Global cancer statistics 2018: GLOBOCAN estimates of incidence and mortality worldwide for 36 cancers in 185 countries. CA Cancer J Clin. 2018;68(6):394–424.
2. Chow LQM. Head and Neck Cancer. N Engl J Med. 2020;382(1):60–72.
3. Skarsgard DP, Groome PA, Mackillop WJ, Zhou S, Rothwell D, Dixon PF, et al. Cancers of the upper aerodigestive tract in Ontario, Canada, and the United States. Cancer. 2000;88(7):1728–38.
4. Simard EP, Torre LA, Jemal A. International trends in head and neck cancer incidence rates: differences by country, sex and anatomic site. Oral Oncol. 2014;50(5):387–403.
5. Wyss A, Hashibe M, Chuang SC, Lee YC, Zhang ZF, Yu GP, et al. Cigarette, cigar, and pipe smoking and the risk of head and neck cancers: pooled analysis in the International Head and Neck Cancer Epidemiology Consortium. Am J Epidemiol. 2013;178(5):679–90.
6. Freedman ND, Schatzkin A, Leitzmann MF, Hollenbeck AR, Abnet CC. Alcohol and head and neck cancer risk in a prospective study. Br J Cancer. 2007;96(9):1469–74.
7. Michaud DS, Langevin SM, Eliot M, Nelson HH, Pawlita M, McClean MD, et al. High-risk HPV types and head and neck cancer. Int J Cancer. 2014;135(7):1653–61.
8. Du E, Mazul AL, Farquhar D, Brennan P, Anantharaman D, Abedi-Ardekani B, et al. Long-term Survival in Head and Neck Cancer: Impact of Site, Stage, Smoking, and Human Papillomavirus Status. Laryngoscope. 2019;129(11):2506–13.
9. Payakachat N, Ounpraseuth S, Suen JY. Late complications and long-term quality of life for survivors (> 5 years) with history of head and neck cancer. Head Neck. 2013;35(6):819–25.
10. Duhrsen L, Hartfuss S, Hirsch D, Geiger S, Maire CL, Sedlacik J, et al. Preclinical analysis of human mesenchymal stem cells: tumor tropism and therapeutic efficiency of local HSV-TK suicide gene therapy in glioblastoma. Oncotarget. 2019;10(58):6049–61.
11. Vegh I, Grau M, Gracia M, Grande J, de la Torre P, Flores AI. Decidua mesenchymal stem cells migrated toward mammary tumors in vitro and in vivo affecting tumor growth and tumor development. Cancer Gene Ther. 2013;20(1):8–16.
12. McGrail DJ, Ghosh D, Quach ND, Dawson MR. Differential mechanical response of mesenchymal stem cells and fibroblasts to tumor-secreted soluble factors. PLoS One. 2012;7(3):e33248.
13. Menon LG, Picinich S, Koneru R, Gao H, Lin SY, Koneru M, et al. Differential gene expression associated with migration of mesenchymal stem cells to conditioned medium from tumor cells or bone marrow cells. Stem Cells. 2007;25(2):520–8.
14. Bitsika V, Roubelakis MG, Zagoura D, Trohatou O, Makridakis M, Pappa KI, et al. Human amniotic fluid-derived mesenchymal stem cells as therapeutic vehicles: a novel approach for the treatment of bladder cancer. Stem Cells Dev. 2012;21(7):1097–111.
15. Wang H, Cao F, De A, Cao Y, Contag C, Gambhir SS, et al. Trafficking mesenchymal stem cell engraftment and differentiation in tumor-bearing mice by bioluminescence imaging. Stem Cells.

2009;27(7):1548–58.

16. Kidd S, Spaeth E, Dembinski JL, Dietrich M, Watson K, Klopp A, et al. Direct evidence of mesenchymal stem cell tropism for tumor and wounding microenvironments using in vivo bioluminescent imaging. Stem Cells. 2009;27(10):2614–23.
17. Doucette T, Rao G, Yang Y, Gumin J, Shinojima N, Bekele BN, et al. Mesenchymal stem cells display tumor-specific tropism in an RCAS/Ntv-a glioma model. Neoplasia. 2011;13(8):716–25.
18. Melzer C, Yang Y, Hass R. Interaction of MSC with tumor cells. Cell Commun Signal. 2016;14(1):20.
19. Ramasamy R, Lam EW, Soeiro I, Tisato V, Bonnet D, Dazzi F. Mesenchymal stem cells inhibit proliferation and apoptosis of tumor cells: impact on in vivo tumor growth. Leukemia. 2007;21(2):304–10.
20. Lee HY, Hong IS. Double-edged sword of mesenchymal stem cells: Cancer-promoting versus therapeutic potential. Cancer Sci. 2017;108(10):1939–46.
21. Ljujic B, Milovanovic M, Volarevic V, Murray B, Bugarski D, Przyborski S, et al. Human mesenchymal stem cells creating an immunosuppressive environment and promote breast cancer in mice. Sci Rep. 2013;3:2298.
22. Xu Q, Wang L, Li H, Han Q, Li J, Qu X, et al. Mesenchymal stem cells play a potential role in regulating the establishment and maintenance of epithelial-mesenchymal transition in MCF7 human breast cancer cells by paracrine and induced autocrine TGF-beta. Int J Oncol. 2012;41(3):959–68.
23. Nomoto-Kojima N, Aoki S, Uchihashi K, Matsunobu A, Koike E, Ootani A, et al. Interaction between adipose tissue stromal cells and gastric cancer cells in vitro. Cell Tissue Res. 2011;344(2):287–98.
24. Zhu W, Huang L, Li Y, Qian H, Shan X, Yan Y, et al. Mesenchymal stem cell-secreted soluble signaling molecules potentiate tumor growth. Cell Cycle. 2011;10(18):3198–207.
25. Lin JT, Wang JY, Chen MK, Chen HC, Chang TH, Su BW, et al. Colon cancer mesenchymal stem cells modulate the tumorigenicity of colon cancer through interleukin 6. Exp Cell Res. 2013;319(14):2216–29.
26. Vallabhaneni KC, Penfornis P, Dhule S, Guillonneau F, Adams KV, Mo YY, et al. Extracellular vesicles from bone marrow mesenchymal stem/stromal cells transport tumor regulatory microRNA, proteins, and metabolites. Oncotarget. 2015;6(7):4953–67.
27. Waterman RS, Henkle SL, Betancourt AM. Mesenchymal stem cell 1 (MSC1)-based therapy attenuates tumor growth whereas MSC2-treatment promotes tumor growth and metastasis. PLoS One. 2012;7(9):e45590.
28. Ho IA, Toh HC, Ng WH, Teo YL, Guo CM, Hui KM, et al. Human bone marrow-derived mesenchymal stem cells suppress human glioma growth through inhibition of angiogenesis. Stem Cells. 2013;31(1):146–55.
29. Chao KC, Yang HT, Chen MW. Human umbilical cord mesenchymal stem cells suppress breast cancer tumourigenesis through direct cell-cell contact and internalization. J Cell Mol Med. 2012;16(8):1803–15.

30. Lu YR, Yuan Y, Wang XJ, Wei LL, Chen YN, Cong C, et al. The growth inhibitory effect of mesenchymal stem cells on tumor cells in vitro and in vivo. Cancer Biol Ther. 2008;7(2):245–51.
31. Sun B, Roh KH, Park JR, Lee SR, Park SB, Jung JW, et al. Therapeutic potential of mesenchymal stromal cells in a mouse breast cancer metastasis model. Cytotherapy. 2009;11(3):289–98. 1 p following 98.
32. Wang ML, Pan CM, Chiou SH, Chen WH, Chang HY, Lee OK, et al. Oncostatin m modulates the mesenchymal-epithelial transition of lung adenocarcinoma cells by a mesenchymal stem cell-mediated paracrine effect. Cancer Res. 2012;72(22):6051–64.
33. de la Garza-Rodea AS, van der Velde-van Dijke I, Boersma H, Goncalves MA, van Bekkum DW, de Vries AA, et al. Myogenic properties of human mesenchymal stem cells derived from three different sources. Cell Transplant. 2012;21(1):153–73.
34. Krampera M, Marconi S, Pasini A, Galie M, Rigotti G, Mosna F, et al. Induction of neural-like differentiation in human mesenchymal stem cells derived from bone marrow, fat, spleen and thymus. Bone. 2007;40(2):382–90.
35. Pirjali T, Azarpira N, Ayatollahi M, Aghdaie MH, Geramizadeh B, Talai T. Isolation and Characterization of Human Mesenchymal Stem Cells Derived from Human Umbilical Cord Wharton's Jelly and Amniotic Membrane. Int J Organ Transplant Med. 2013;4(3):111–6.
36. Gronthos S, Mankani M, Brahim J, Robey PG, Shi S. Postnatal human dental pulp stem cells (DPSCs) in vitro and in vivo. Proc Natl Acad Sci U S A. 2000;97(25):13625–30.
37. Belmar-Lopez C, Mendoza G, Oberg D, Burnet J, Simon C, Cervello I, et al. Tissue-derived mesenchymal stromal cells used as vehicles for anti-tumor therapy exert different in vivo effects on migration capacity and tumor growth. BMC Med. 2013;11:139.
38. Sasso RC, LeHuec JC, Shaffrey C, Spine Interbody Research G. Iliac crest bone graft donor site pain after anterior lumbar interbody fusion: a prospective patient satisfaction outcome assessment. J Spinal Disord Tech. 2005;18(Suppl):77–81.
39. Alge DL, Zhou D, Adams LL, Wyss BK, Shadday MD, Woods EJ, et al. Donor-matched comparison of dental pulp stem cells and bone marrow-derived mesenchymal stem cells in a rat model. J Tissue Eng Regen Med. 2010;4(1):73–81.
40. Hilkens P, Gervois P, Fanton Y, Vanormelingen J, Martens W, Struys T, et al. Effect of isolation methodology on stem cell properties and multilineage differentiation potential of human dental pulp stem cells. Cell Tissue Res. 2013;353(1):65–78.
41. Liekens S, Bronckaers A, Belleri M, Bugatti A, Sienaert R, Ribatti D, et al. The thymidine phosphorylase inhibitor 5'-O-tritylinosine (KIN59) is an antiangiogenic multitarget fibroblast growth factor-2 antagonist. Mol Cancer Ther. 2012;11(4):817–29.
42. Dittmer A, Hohlfeld K, Lutzkendorf J, Muller LP, Dittmer J. Human mesenchymal stem cells induce E-cadherin degradation in breast carcinoma spheroids by activating ADAM10. Cell Mol Life Sci. 2009;66(18):3053–65.

43. Potente M, Gerhardt H, Carmeliet P. Basic and therapeutic aspects of angiogenesis. Cell. 2011;146(6):873–87.
44. Bronckaers A, Hilkens P, Martens W, Gervois P, Ratajczak J, Struys T, et al. Mesenchymal stem/stromal cells as a pharmacological and therapeutic approach to accelerate angiogenesis. Pharmacol Ther. 2014;143(2):181–96.
45. Hanyu S, Sakuma K, Tanaka A. A Study on the Effect of Human Dental Pulp Stem Cell Conditioned Medium on Human Oral Squamous Cell Carcinoma Cell Lines. J Hard Tissue Biol. 2019;28(3):281–8.
46. Zurmukhtashvili M, Machavariani A, Dugashvili G, Grdzelidze T, Gogilashvili K, Menabde G, et al. Mesenchymal stem cell transplantation attenuates growth of chemotherapy treated oral squamous cell carcinoma in an animal model. J Oral Pathol Med. 2020.
47. Lim YS, Lee JC, Lee YS, Lee BJ, Wang SG. Growth Inhibitory Effect of Palatine Tonsil-derived Mesenchymal Stem Cells on Head and Neck Squamous Cell Carcinoma Cells. Clin Exp Otorhinolaryngol. 2012;5(2):86–93.
48. Zhou S, Cecere R, Philip A. CD109 released from human bone marrow mesenchymal stem cells attenuates TGF-beta-induced epithelial to mesenchymal transition and stemness of squamous cell carcinoma. Oncotarget. 2017;8(56):95632–47.
49. Scherzed A, Hackenberg S, Froelich K, Kessler M, Koehler C, Hagen R, et al. BMSC enhance the survival of paclitaxel treated squamous cell carcinoma cells in vitro. Cancer Biol Ther. 2011;11(3):349–57.
50. Scherzad A, Steber M, Gehrke T, Rak K, Froelich K, Schendzielorz P, et al. Human mesenchymal stem cells enhance cancer cell proliferation via IL-6 secretion and activation of ERK1/2. Int J Oncol. 2015;47(1):391–7.
51. Liu C, Feng X, Wang B, Wang X, Wang C, Yu M, et al. Bone marrow mesenchymal stem cells promote head and neck cancer progression through Periostin-mediated phosphoinositide 3-kinase/Akt/mammalian target of rapamycin. Cancer Sci. 2018;109(3):688–98.
52. Wessely A, Waltera A, Reichert TE, Stockl S, Grassel S, Bauer RJ. Induction of ALP and MMP9 activity facilitates invasive behavior in heterogeneous human BMSC and HNSCC 3D spheroids. FASEB J. 2019;33(11):11884–93.
53. Scherzed A, Hackenberg S, Radeloff A, Froelich K, Rak K, Hagen R, et al. Human mesenchymal stem cells promote cancer motility and cytokine secretion in vitro. Cells Tissues Organs. 2013;198(5):327–37.
54. Rosland GV, Svendsen A, Torsvik A, Sobala E, McCormack E, Immervoll H, et al. Long-term cultures of bone marrow-derived human mesenchymal stem cells frequently undergo spontaneous malignant transformation. Cancer Res. 2009;69(13):5331–9.
55. Liu J, Zhang Y, Bai L, Cui X, Zhu J. Rat bone marrow mesenchymal stem cells undergo malignant transformation via indirect co-cultured with tumour cells. Cell Biochem Funct. 2012;30(8):650–6.
56. Tang H, Chu Y, Huang Z, Cai J, Wang Z. The metastatic phenotype shift towards myofibroblast of adipose-derived mesenchymal stem cells promotes ovarian cancer progression. Carcinogenesis.

2019.

57. Dhar K, Dhar G, Majumder M, Haque I, Mehta S, Van Veldhuizen PJ, et al. Tumor cell-derived PDGF-B potentiates mouse mesenchymal stem cells-pericytes transition and recruitment through an interaction with NRP-1. Mol Cancer. 2010;9:209.
58. Gu W, Hong X, Le Bras A, Nowak WN, Issa Bhaloo S, Deng J, et al. Smooth muscle cells differentiated from mesenchymal stem cells are regulated by microRNAs and suitable for vascular tissue grafts. J Biol Chem. 2018;293(21):8089–102.
59. Li W, Zhang X, Wu F, Zhou Y, Bao Z, Li H, et al. Gastric cancer-derived mesenchymal stromal cells trigger M2 macrophage polarization that promotes metastasis and EMT in gastric cancer. Cell Death Dis. 2019;10(12):918.
60. Patel SA, Meyer JR, Greco SJ, Corcoran KE, Bryan M, Rameshwar P. Mesenchymal stem cells protect breast cancer cells through regulatory T cells: role of mesenchymal stem cell-derived TGF-beta. J Immunol. 2010;184(10):5885–94.
61. Nishimura K, Semba S, Aoyagi K, Sasaki H, Yokozaki H. Mesenchymal stem cells provide an advantageous tumor microenvironment for the restoration of cancer stem cells. Pathobiology. 2012;79(6):290–306.
62. Liu S, Ginestier C, Ou SJ, Clouthier SG, Patel SH, Monville F, et al. Breast cancer stem cells are regulated by mesenchymal stem cells through cytokine networks. Cancer Res. 2011;71(2):614–24.
63. Yulyana Y, Ho IA, Sia KC, Newman JP, Toh XY, Endaya BB, et al. Paracrine factors of human fetal MSCs inhibit liver cancer growth through reduced activation of IGF-1R/PI3K/Akt signaling. Mol Ther. 2015;23(4):746–56.
64. Rosenberger L, Ezquer M, Lillo-Vera F, Pedraza PL, Ortuzar MI, Gonzalez PL, et al. Stem cell exosomes inhibit angiogenesis and tumor growth of oral squamous cell carcinoma. Sci Rep. 2019;9(1):663.
65. Hernanda PY, Pedroza-Gonzalez A, van der Laan LJ, Broker ME, Hoogduijn MJ, Ijzermans JN, et al. Tumor promotion through the mesenchymal stem cell compartment in human hepatocellular carcinoma. Carcinogenesis. 2013;34(10):2330–40.
66. Al-toub M, Almusa A, Almajed M, Al-Nbaheen M, Kassem M, Aldahmash A, et al. Pleiotropic effects of cancer cells' secreted factors on human stromal (mesenchymal) stem cells. Stem Cell Res Ther. 2013;4(5):114.
67. Wang J, Zhu L, Chen X, Huang R, Wang S, Dong P. Human Bone Marrow Mesenchymal Stem Cells Functionalized by Hybrid Baculovirus-Adeno-Associated Viral Vectors for Targeting Hypopharyngeal Carcinoma. Stem Cells Dev. 2019;28(8):543–53.
68. Scherzed A, Hackenberg S, Froelich K, Rak K, Schendzielorz P, Gehrke T, et al. The differentiation of hMSCs counteracts their migration capability and pro-angiogenic effects in vitro. Oncol Rep. 2016;35(1):219–26.
69. Oloyo AK, Ambele MA, Pepper MS. Contrasting Views on the Role of Mesenchymal Stromal/Stem Cells in Tumour Growth: A Systematic Review of Experimental Design. Adv Exp Med Biol. 2018;1083:103–24.

70. Barbash IM, Chouraqui P, Baron J, Feinberg MS, Etzion S, Tessone A, et al. Systemic delivery of bone marrow-derived mesenchymal stem cells to the infarcted myocardium: feasibility, cell migration, and body distribution. Circulation. 2003;108(7):863–8.
71. Suchanek J, Soukup T, Visek B, Ivancakova R, Kucerova L, Mokry J. Dental pulp stem cells and their characterization. Biomed Pap Med Fac Univ Palacky Olomouc Czech Repub. 2009;153(1):31–5.
72. Lan X, Sun Z, Chu C, Boltze J, Li S. Dental Pulp Stem Cells: An Attractive Alternative for Cell Therapy in Ischemic Stroke. Front Neurol. 2019;10:824.
73. Doerschuk CM, Beyers N, Coxson HO, Wiggs B, Hogg JC. Comparison of neutrophil and capillary diameters and their relation to neutrophil sequestration in the lung. J Appl Physiol (1985). 1993;74(6):3040–5.
74. Schrepfer S, Deuse T, Reichenspurner H, Fischbein MP, Robbins RC, Pelletier MP. Stem cell transplantation: the lung barrier. Transplant Proc. 2007;39(2):573-6.
75. Bianchi G, Morandi F, Cilli M, Daga A, Bocelli-Tyndall C, Gambini C, et al. Close interactions between mesenchymal stem cells and neuroblastoma cell lines lead to tumor growth inhibition. PLoS One. 2012;7(10):e48654.
76. Fischer UM, Harting MT, Jimenez F, Monzon-Posadas WO, Xue H, Savitz SI, et al. Pulmonary passage is a major obstacle for intravenous stem cell delivery: the pulmonary first-pass effect. Stem Cells Dev. 2009;18(5):683–92.
77. Zielske SP, Livant DL, Lawrence TS. Radiation increases invasion of gene-modified mesenchymal stem cells into tumors. Int J Radiat Oncol Biol Phys. 2009;75(3):843–53.
78. Lee RH, Pulin AA, Seo MJ, Kota DJ, Ylostalo J, Larson BL, et al. Intravenous hMSCs improve myocardial infarction in mice because cells embolized in lung are activated to secrete the anti-inflammatory protein TSG-6. Cell Stem Cell. 2009;5(1):54–63.
79. Bazhanov N, Ylostalo JH, Bartosh TJ, Tiblow A, Mohammadipoor A, Foskett A, et al. Intraperitoneally infused human mesenchymal stem cells form aggregates with mouse immune cells and attach to peritoneal organs. Stem Cell Res Ther. 2016;7:27.
80. Altanerova U, Benejova K, Altanerova V, Tyciakova S, Rychly B, Szomolanyi P, et al. Dental pulp mesenchymal stem/stromal cells labeled with iron sucrose release exosomes and cells applied intra-nasally migrate to intracerebral glioblastoma. Neoplasma. 2016;63(6):925–33.
81. Schweizer MT, Wang H, Bivalacqua TJ, Partin AW, Lim SJ, Chapman C, et al. A Phase I Study to Assess the Safety and Cancer-Homing Ability of Allogeneic Bone Marrow-Derived Mesenchymal Stem Cells in Men with Localized Prostate Cancer. Stem Cells Transl Med. 2019;8(5):441–9.
82. Olson A, Marini F, Westin S, Coleman R, Thall P, Al Jhadhami V, et al. A Phase I Trial of Mesenchymal Stem Cells Transfected with a Plasmid Secreting Interferon Beta in Advanced Ovarian Cancer. Biol Blood Marrow Transplant. 2018;24.
83. Dvorak HF. Tumors: wounds that do not heal. Similarities between tumor stroma generation and wound healing. N Engl J Med. 1986;315(26):1650–9.

84. Spaeth E, Klopp A, Dembinski J, Andreeff M, Marini F. Inflammation and tumor microenvironments: defining the migratory itinerary of mesenchymal stem cells. Gene Ther. 2008;15(10):730–8.
85. Klopp AH, Spaeth EL, Dembinski JL, Woodward WA, Munshi A, Meyn RE, et al. Tumor irradiation increases the recruitment of circulating mesenchymal stem cells into the tumor microenvironment. Cancer Res. 2007;67(24):11687–95.
86. Kim SM, Oh JH, Park SA, Ryu CH, Lim JY, Kim DS, et al. Irradiation enhances the tumor tropism and therapeutic potential of tumor necrosis factor-related apoptosis-inducing ligand-secreting human umbilical cord blood-derived mesenchymal stem cells in glioma therapy. Stem Cells. 2010;28(12):2217–28.
87. Akimoto K, Kimura K, Nagano M, Takano S, To'a Salazar G, Yamashita T, et al. Umbilical cord blood-derived mesenchymal stem cells inhibit, but adipose tissue-derived mesenchymal stem cells promote, glioblastoma multiforme proliferation. Stem Cells Dev. 2013;22(9):1370–86.
88. Subramanian A, Shu-Uin G, Kae-Siang N, Gauthaman K, Biswas A, Choolani M, et al. Human umbilical cord Wharton's jelly mesenchymal stem cells do not transform to tumor-associated fibroblasts in the presence of breast and ovarian cancer cells unlike bone marrow mesenchymal stem cells. J Cell Biochem. 2012;113(6):1886–95.
89. Grisendi G, Bussolari R, Cafarelli L, Petak I, Rasini V, Veronesi E, et al. Adipose-derived mesenchymal stem cells as stable source of tumor necrosis factor-related apoptosis-inducing ligand delivery for cancer therapy. Cancer Res. 2010;70(9):3718–29.
90. Zhang D, Zheng L, Shi H, Chen X, Wan Y, Zhang H, et al. Suppression of peritoneal tumorigenesis by placenta-derived mesenchymal stem cells expressing endostatin on colorectal cancer. Int J Med Sci. 2014;11(9):870–9.
91. Zhang X, Xu W, Qian H, Zhu W, Zhang R. Mesenchymal stem cells modified to express lentivirus TNF-alpha Tumstatin(45–132) inhibit the growth of prostate cancer. J Cell Mol Med. 2011;15(2):433–44.
92. Salehi H, Al-Arag S, Middendorp E, Gergely C, Cuisinier F, Orti V. Dental pulp stem cells used to deliver the anticancer drug paclitaxel. Stem Cell Res Ther. 2018;9(1):103.

Figures

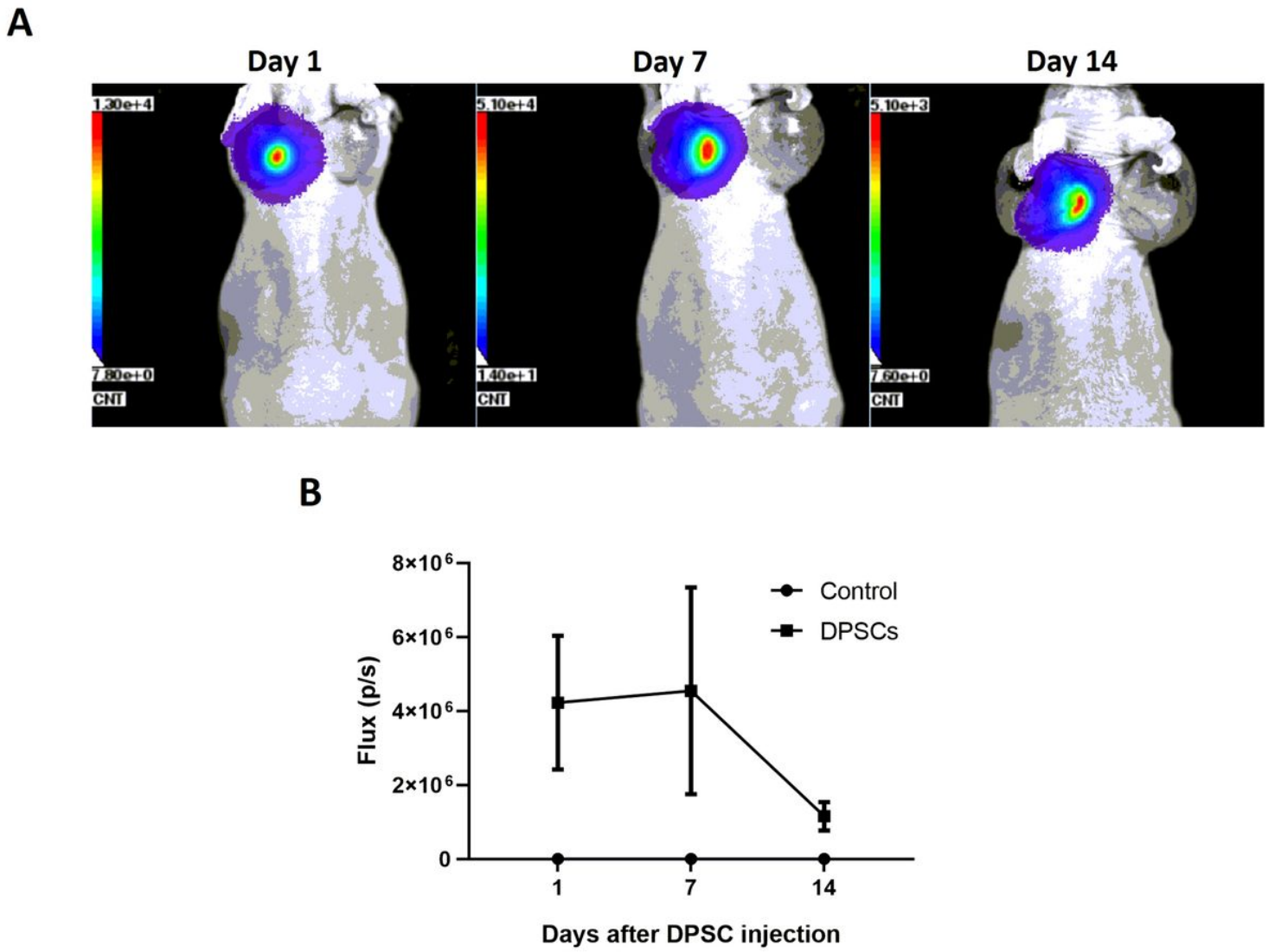

Figure 1

Survival of DPSCs after their injection in HNSCC xenografts. FaDu tumour xenografts were induced in the contralateral flanks of mice. Ten days later, Fluc-expressing DPSCs or control medium was injected. Representative BLI pictures of DPSC presence are shown after 1, 7 and 14 days (A). Quantification of the total photon flux (p/s) in control and DPSC-injected tumours indicated the persistence of DPSCs in the xenografts, with a decline at day 14 (B, n = 6). Data are expressed as mean ± S.E.M.

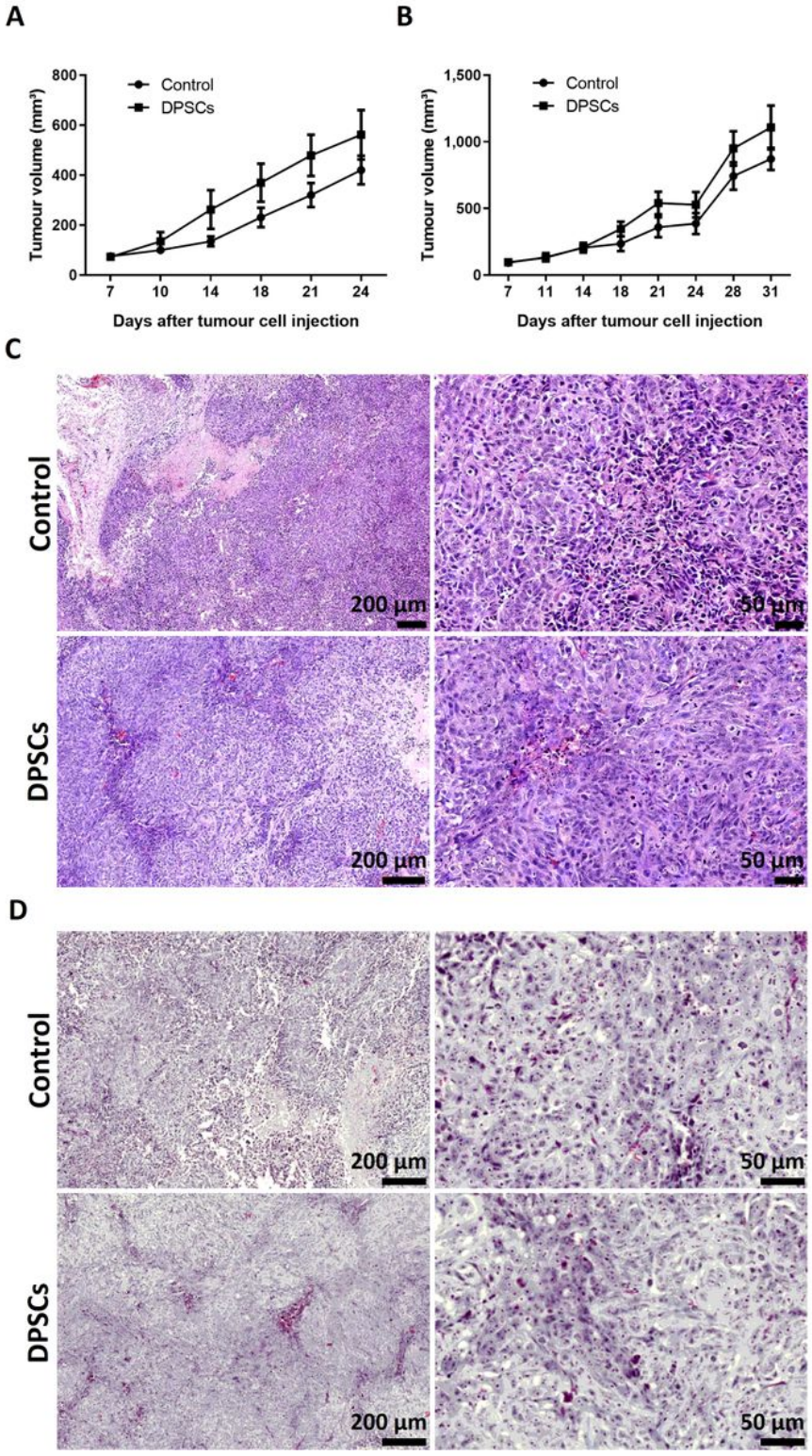

Figure 2

No significant effect of DPSCs on HNSCC morphology and growth. FaDu xenografts were induced and injected with DPSCs or medium after 10 days. Mice received either two tumours (A, n = 20, 4 DPSC donors) or one tumour (B, n = 8, 2 DPSC donors). Tumour growth was measured over time, unveiling no significant influence of the injected DPSCs. Tumour volume (mm³) is displayed as mean ± S.E.M. and statistically analysed by two-way ANOVA and Sidak's multiple comparisons test (A–B). The general

morphology of the tumours from experiment A was compared by H&E (C) or Masson's trichrome (D) staining at day 24.

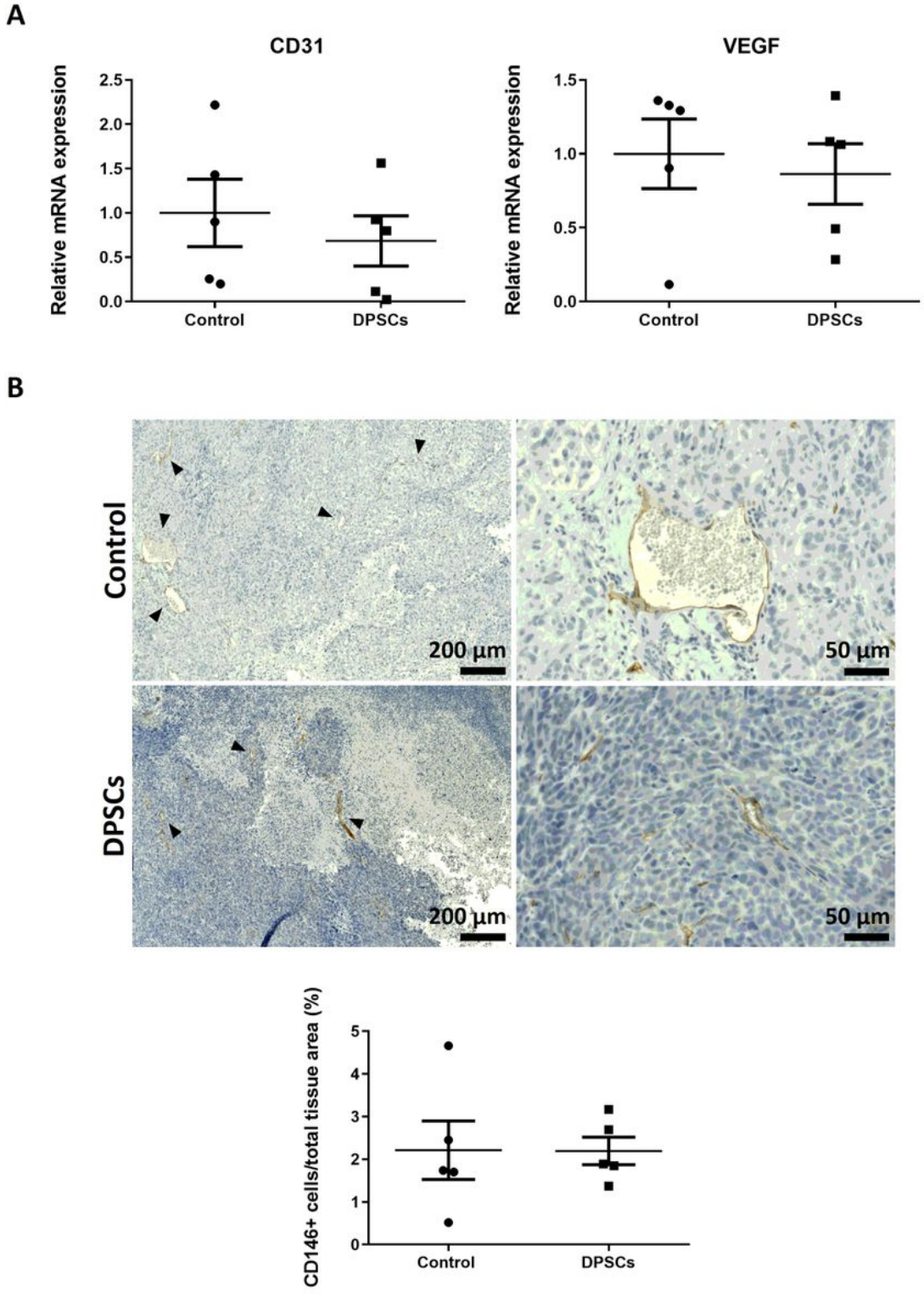

Figure 3

DPSCs did not influence neovascularization in mouse HNSCC xenografts. Vascularization of FaDu xenografts injected with DPSCs or medium (control) was evaluated by qRT-PCR for CD31 and VEGF after 24 days. Similar expression levels were measured for control and DPSC-injected tumours (A, n = 5). The

number of blood vessels was analysed by immunohistochemistry for CD146. Representative pictures of DPSC-injected or control xenografts show the presence of endothelial cells surrounding the blood vessels (indicated by arrows). Quantification of these cells in function of the total tissue area revealed no significant effect of DPSCs on tumour angiogenesis (B, n = 5). Data are presented as mean ± S.E.M. and compared by the Mann-Whitney U test.

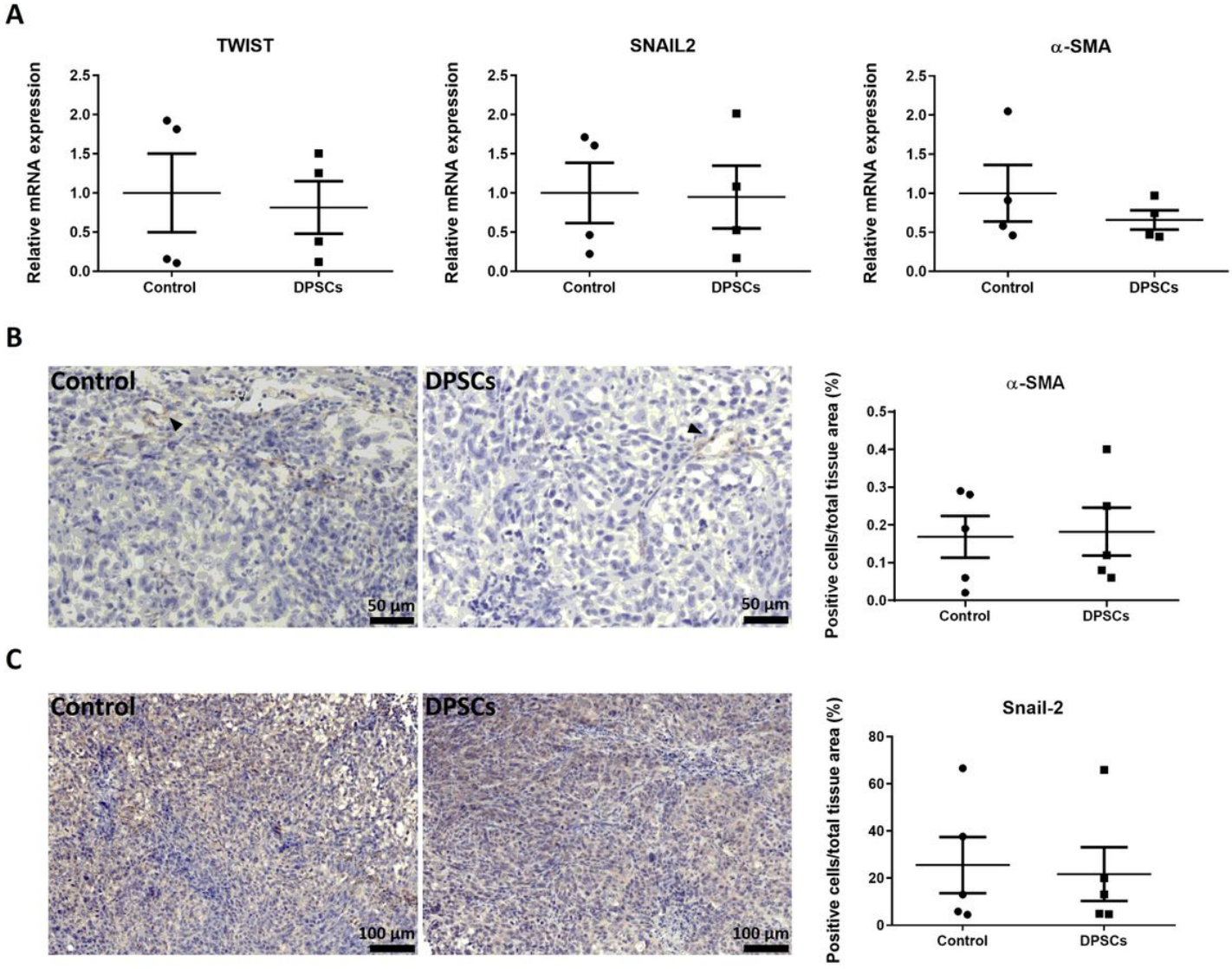

Figure 4

DPSCs have no effect on EMT in HNSCC grafts. Expression levels of TWIST, SNAIL2 and α-SMA were measured in control and DPSC-injected FaDu xenografts. No differences in EMT-related gene expression were detected (A, n = 4). Protein levels of α-SMA (B) and Snail-2 (C) were evaluated in tumour sections by immunohistochemistry. The percentage of positive cells was quantified, but was not changed in DPSC-injected tumours as analysed by the Mann-Whitney U test (n = 5). Data are mentioned as mean ± S.E.M.

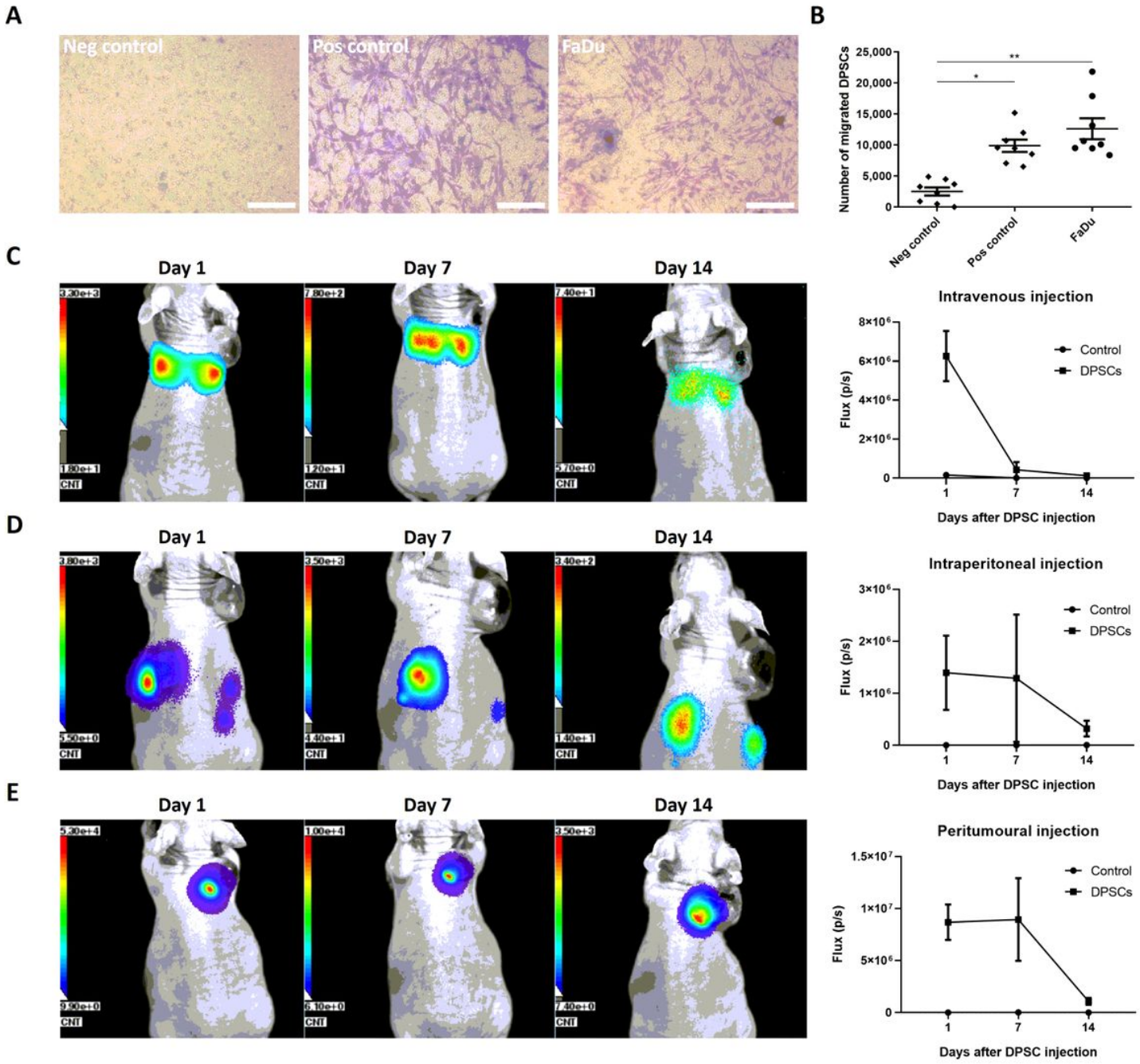

Figure 5

DPSCs migrate towards HNSCC cells in vitro, which could not be confirmed in vivo. DPSC migration in vitro was assessed with the transwell assay. After 24 h, DPSCs were able to migrate towards FaDu cells. Transmigrated DPSCs were visualized and quantified by crystal violet (A) and calcein (B, n = 8) staining, respectively. In addition, in vivo stem cell homing was assessed. DPSCs were injected intravenously (C), intraperitoneally (D) or peritumourally (E). DPSC survival and biodistribution were monitored over time using BLI. Injected DPSCs were detectable during 14 days, with a gradual decrease in signal intensity in time, but stem cell migration could not be observed (n = 3). Scale bars represent 200 µm and quantitative data are expressed as mean ± S.E.M. * $p < 0.001$, ** $p < 0.0001$ as determined by one-way ANOVA combined with Dunnett's multiple comparisons test.

Supplementary Files

This is a list of supplementary files associated with this preprint. Click to download.

- GMerckxAdditionalFile1.pdf